EXPERIMENTAL EQUIPMENT STATUS

Facilities in Operation

Isotope Production Area and Off-Line Radiochemistry and Decay Spectroscopy Laboratory

The isotope production area is presently used for a variety of experiments with high-intensity beams using both charged particles and high-energy secondary neutrons. The target stations located along the beam line can accommodate a variety of experiments, often parasitically. They are: a) He-jet terminal, b) solid target-charged particle irradiation facility, c) an automatic beam degrader, d) a general purpose station, and e) a stopped beam high energy neutron facility. The He-jet system has been built by Prof. E.S. Macias (Washington University) and plans are underway to install it during the summer of 1978 and to look for some nuclei far removed from stability. The charged particle and neutron targets are transported from the isotope production room to the chemistry trailer using a pneumatic rapid transport system. The production of neutron rich nuclei using fast neutrons and the production of neutral pions from proton-nucleus reactions at intermediate energies are typical studies making use of these facilities. The beam degrader and general purpose station have been used extensively for the production of ^{123}I from various targets. A special isotope production facility attaches conveniently to the beam line.

The radiochemistry laboratory is nearing completion with the planned installation of the fume-hood in the next few months. The chemistry trailer also houses the rapid transport receiving terminals for the charged-particle and fast-neutron systems. With the installation of water utilities and the fume-hood, the chem trailer will be ready for radio chemical studies.

The spectroscopy trailer has been used extensively over the past year. Almost all of the off-line counting is performed there. Two multi-channel analyzers are available, a Canberra 8180 and a Nuclear Data 50/50 system. Various Ge(Li) detectors, a KEVEX x-ray detector and a LEPS are used in various experimental configurations. Plans are underway to provide vacuum to both trailers and to eventually perform all off-line α, β and γ counting in this area.

In-Beam γ-Ray Area Thin-Walled Target Chamber

With the aim of reducing the total mass of material in the proximity of the target, a thin-walled target chamber was constructed for use in the in-beam γ-ray area. The chamber is very simple in design, having the form of an elongated cross, made principally from 6.35-cm diameter aluminum tubing (.8mm wall thickness). Two targets and a scintillator viewer may be manually positioned in the cross center. No direct comparison has as yet been made of the γ-ray backgrounds resulting from beam tunes through this and the older more massive chamber. Use of the new chamber has, however, significantly helped the background problem in at least one low-yield γ-ray measurement. A further result of the change is that the support system for the chamber in this area was

modified in order to make interchange of the chambers both simple and reproducible in terms of alignment. This also will allow future variations in target and detector configuration to be more easily accommodated.

A Hyper-Pure Germanium Detector Telescope System for Use in the 64" Scattering Chamber

A pair of hyper-pure germanium detector telescopes for general laboratory use in the 64" scattering chamber are currently under construction and test. The telescopes, each capable of stopping up to 100 MeV protons, consist of a 1cm and a 1.5cm deep by 3cm diameter hyper-pure, transmission mounted germanium crystals placed on a liquid nitrogen cryostat located on each arm of the 64" chamber. The telescopes are designed for easy rearrangement of the crystals to meet varying experimental requirements. All four detectors, for example, may be mounted in one telescope to stop protons of up to 160 MeV. Provisions are made for using small area silicon surface barrier detectors in front, and large volume sodium iodide veto detectors behind the telescopes. Solid angle defining apertures of any size are easily mounted in front of the telescopes. A schematic diagram of the telescope system is shown in Fig. 7.

The detectors are enclosed in their own clean vacuum environment pumped by a small CTI 20°K cryopump. Pumping and LN filling are accomplished through flexible metal hoses passing through the lid of the scattering chamber, allowing complete freedom

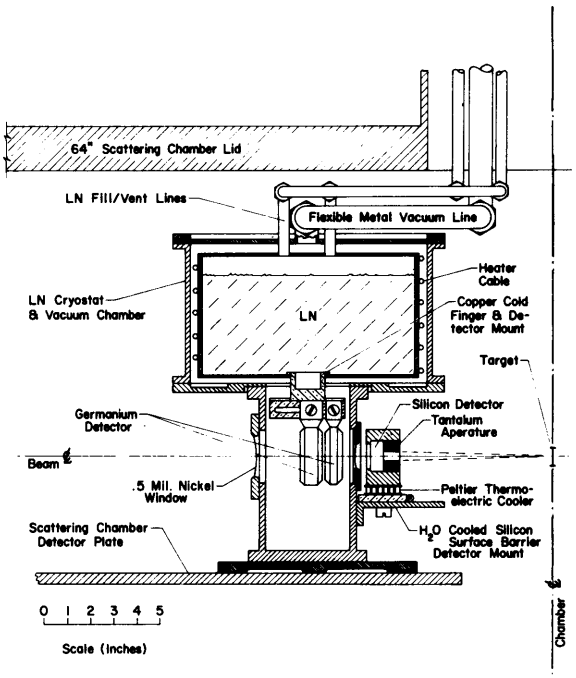

Figure 7. Schematic diagram of a hyper-pure germanium detector telescope for use in the 64" scattering chamber.

of motion of the telescopes on their respective arms. Each telescope may be rotated through 180° about the target position. Scattered particles enter and exit the telescope through .5mil thick nickel foils.

The telescopes may be mounted in any one of five positions of varying distance from the target as determined by dowel pins which are compatible with the locating holes already in the movable arms of the 64" chamber. It is also possible to mount both telescopes on one arm, but only at different distances from the target. Table 6 lists the vital statistics for the detectors and the telescopes, along with a list of the maximum solid angle and minimum usable detector angle vs. distance from the target for the five positions.

The hyper-pure germanium crystals are being made for this laboratory by R. Pehl of the Lawrence Berkeley Laboratory, who is collaborating with us to determine their operating characteristics at IUCF energies. They differ significantly from commercially available detectors of this type in that both electrical contacts are ion implanted. The usual lithium contact is replaced by a phosphorus ion implant, while the positive contact is a boron ion implanted surface. The replacement of the relatively thick lithium surface (≈10μm) by the phosphorus implanted contact is not only important because the detectors will be used in the transmission mode, but because these detectors can readily be stored at room temperature without worry about continual drifting of the lithium. Furthermore, because these are large volume detectors, they are quite easily radiation damaged by both neutrons and charged particles. Experience in our laboratory has shown that a neutron dose of about 10^{10} particles or a charged particle dose of 10^{9} particles at IUCF energies is enough to destroy the resolution of the detectors. This damage can be repaired by annealing the detector at 140°C for 24 hours. The effect this annealing process has on the drifting of a lithium contact has not been measured, but is of concern. The replacement of the lithium contact by the phosphorus contact should solve the problem.

Table 6. Germanium detector properties and telescope geometry.

Germanium Detector Properties

Detector thicknesses:	1.0cm and 1.5cm (2 each)
Detector diameter:	3.0cm
Detector case O.D.:	5.16cm
Detector case I.D.:	2.40cm
Useful detector area:	452mm^2

Telescope Geometry*

Distance from Target (cm)	Max. Solid Angle (msr)	θ_{lab} Min. (deg)
20.0	2.5	11.3
25.0	2.0	9.0
30.0	1.67	7.6
41.0	1.26	5.5
62.5	0.8	3.7

*These calculations were made for each telescope having a 1.0 and a 1.5cm thick detector in tandem for the detection of 18 to 100 MeV protons, and take into account the expected small angle scattering in the detectors.

Several damage/anneal cycles on our existing germanium detector, which has the lithium contact, have shown no deterioration of the detector resolution. This detector is used only as a stopping detector, however, where the boron contact is used as the entrance face.

Construction and testing of the detectors and their housings are in progress. The completed system is expected to be ready for use by the end of April, 1978.

QDDM Spectrograph

The QDDM Spectrograph remained the most frequently used facility for experiments with high energy protons and deuterons. The overall resolution of the system is slowly approaching the design goal of $\Delta E/E = 2 \times 10^{-4}$. A spectrum obtained in a recent inelastic proton scattering experiment is shown in Figure 8. An overall resolution of 35 keV fwhm ($\Delta E/E = 3.5 \times 10^{-4}$) was obtained for extended runs. Nearly equivalent performance of the spectrograph was obtained with 160 MeV protons and 75 MeV deuterons.

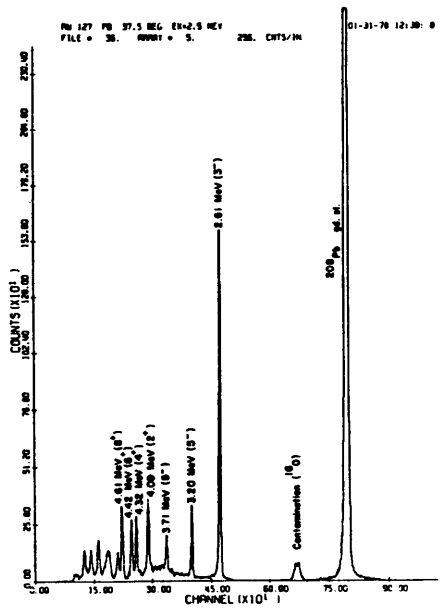

Figure 8. A recent (p,p') spectrum on ^{208}Pb at Tp = 99 MeV; the overall resolution is 35 keV fwhm.

Recent ray tracing measurements indicate that the energy resolution along the length of the focal plane would be improved by a 5 degree rotation of the focal plane detector array. This change, which entails significant modification of the focal plane detector hardware, will not be undertaken until more extensive ray tracing can be carried out to verify the optimal detector angle for a wide range of operating conditions.

Matching the dispersion of the beam line system to that of the spectrograph has met only partial success in improving the resolution routinely achieved in experiments. The dispersions have been matched; however, transmission losses in the beam line system are higher than calculations for the beam transport system indicate they should be. Diagnostic equipment designed to study the coupling of the accelerators to the external beam lines is presently under development. Improvements in the matching of these systems will lead to the availability of higher beam intensities for high resolution experiments.

A system for vacuum transfer of targets has been designed and constructed and is presently undergoing testing. The system will also provide a remotely controlled motor drive for target changing.

Additional improvements to the spectrograph system include design work for a new entrance slit system. Features of the new design include the ability to move the spectrograph to smaller angles with the external Faraday cup and the possibility of using slits specifically tailored to a given experiment.

Photographs of a new heavy-ion detector which attaches to the focal plane of the QDDM spectrograph are shown in Figure 9. The properties of this detector and its use in preliminary studies of the (^{6}Li,^{8}B) reaction are discussed in Part 2 of this Annual Report (see W. Gray et al., p.54).

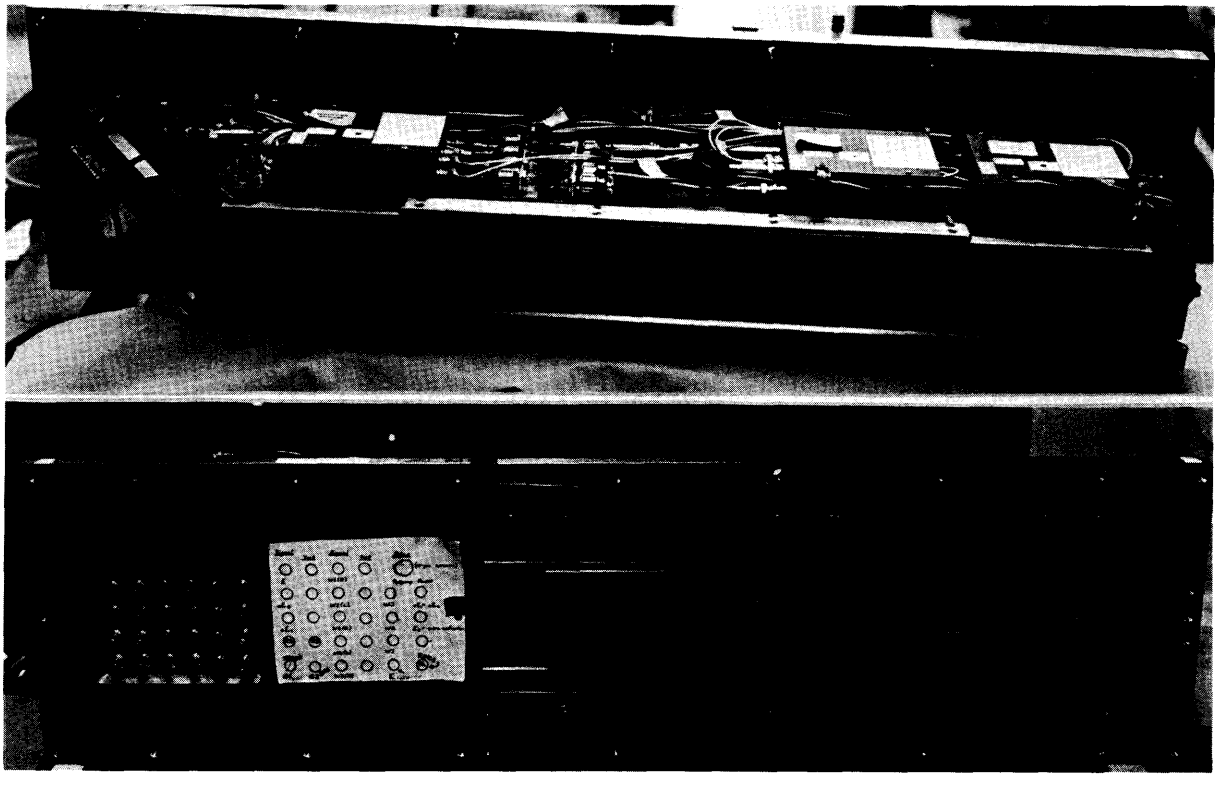

Figure 9. New heavy ion detector which attaches to the focal plane of the QDDM spectrograph. Ions enter the chamber through the ≃ ½ mil thick Kapton window visible in the lower view. The active region of the ion chamber and part of the wire grid planes are visible in the top photograph, which was taken from the back (downstream) side with the gas containment box removed.

$D\bar{D}$ Pion Spectrometer

A miniature non-dispersive $D\bar{D}$ magnetic spectrometer has been constructed to study nuclear charged-pion production very near threshold. The device was designed to be placed inside the 64 inch general purpose scattering chamber on one of its movable arms. A schematic drawing of the spectrometer is shown in Figure 10 and the device is shown in place in Figure 11. The basic properties of the $D\bar{D}$ are outlined in Table 7.

The detector holder is located in a lead castle and is designed to hold up to three standard silicon surface barrier detectors. A typical detector stack consists of a 100 μm Al absorber and a 10 mil plastic scintillator followed by a

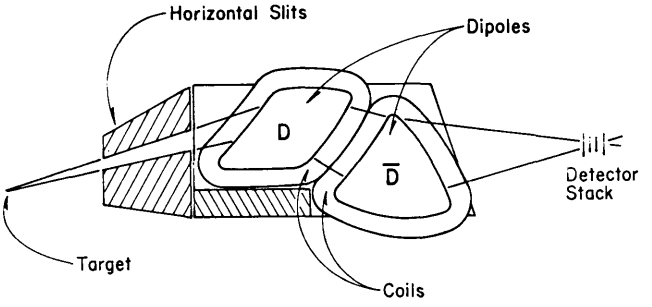

Figure 10. Schematic representation of the $D\bar{D}$ pion spectrometer.

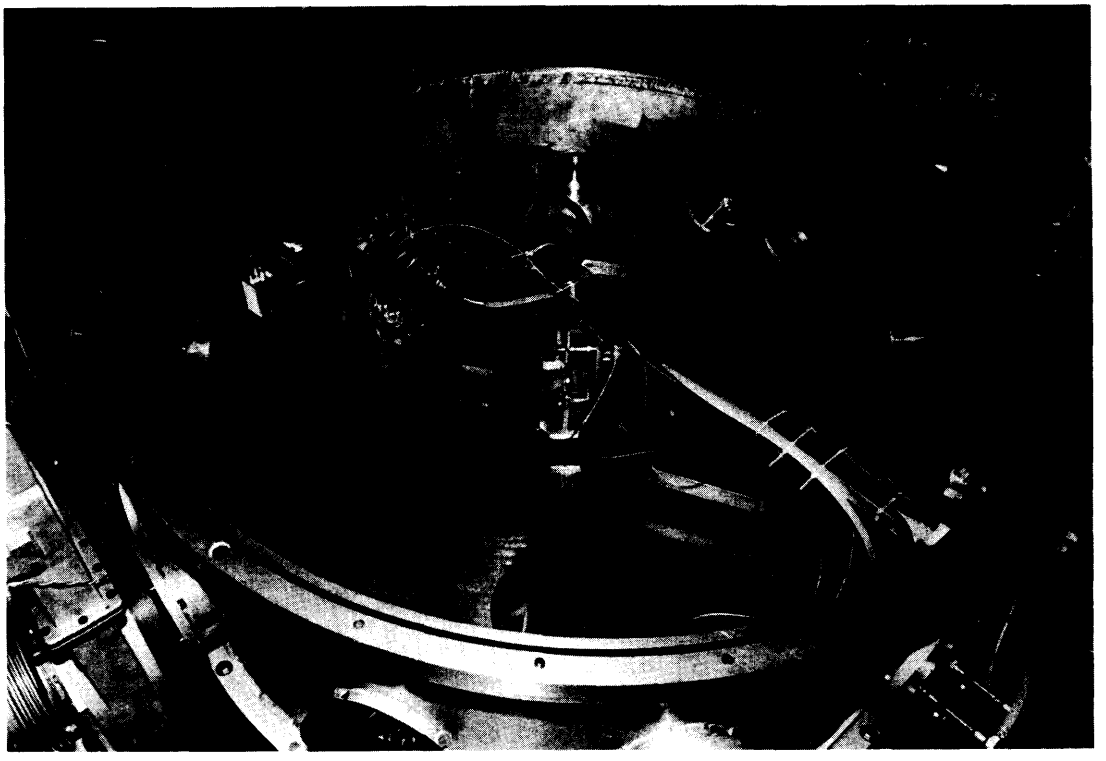

Figure 11. Photograph of the $D\bar{D}$ pion spectrometer inside the 64" scattering chamber. The beam enters the chamber from the upper right hand corner.

silicon stack consisting of a 200 μm ΔE detector, a 5000 μm stopping detector and a large area veto detector. This detector stack is suitable for detecting 4→12 MeV pions. Other detector stacks can be assembled to observe pions with energies above 12 or below 4 MeV. The solid angle as a function of radius of curvature for a detector stack consisting of a 150 mm^2 ΔE and a 100 mm^2 stopping detector is shown in Figure 12 (measured first with alpha particles from a radioactive source and the shape verified with pions).

The projected pion energy range for the QQSP pion spectrograph (see p. 23 of this report) to be constructed in late 1978 is from 8 to 130 MeV; thus the DD̄ pion spectrometer will remain a unique instrument for the study of very near threshold pion production.

Table 7. Properties of the DD̄ pion spectrometer.

Solid angle	3.5 msr (114 mr horizontal, 31 mr vertical)
P_{max}/P_{min}	1.5
Angular range	17-163 deg
Orbit radii	15-23 cm
Flight path	77 cm
Focal plane	non-dispersed (approx. 1.3 x 1.3 cm maximum)
Magnet gap	1.0 cm
Maximum field strength	11 Kg
Maximum pion energy	19 MeV
(11 Kg and rho = 23 cm)	

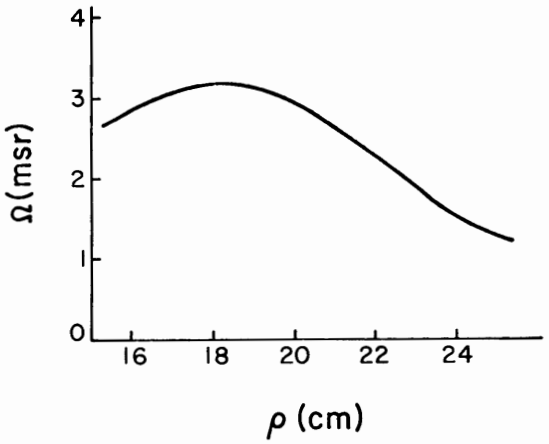

Figure 12. Solid angle of the DD̄ spectrometer as a function of radius of curvature.

Neutron Detectors *

Neutron spectroscopy is complicated by the fact that the interactions by which we detect neutrons do not leave signals proportional to the incident energy. Therefore, we resort to using the *time* of the signal as the indicator of the neutron energy. Even with state-of-the-art timing, flight paths as long as 100 meters are required for adequate energy resolution, bringing on two new problems: 1) It is not practical to swing the detector around the target for angular distributions. We solve this with a beam swinger. 2) Solid angles are unreasonably small. We solve this by developing large detectors.

To grasp the magnitude of the second problem consider that scattering chamber experiments use

solid angles of about one millisterradian, but at 100 m that implies a detector area of $10m^2$! Thus, the detector development imperative is to make detectors as large as possible without degrading the time resolution.

The detectors consist of plastic scintillators coupled to conventional, fast photomultiplier tubes. We limit the cross sectional dimension to that which can be conveniently coupled to the phototubes; our most successful detectors have 15 cm x 15 cm cross sections coupled with tapered light pipes to 5-in. phototubes (these have 11-cm diameter photocathodes).

The scintillators are 1 m long and two different approaches have been used to compensate for transit time spreads over the length. The Kent State group has built detectors with phototubes at both ends and electronics to measure the mean time of light arrival at the two ends. The scintillator is oriented transversely to the flight path. The Oak Ridge-Ohio University group has built detectors[1,2] that employ a single phototube and a tilted scintillator axis. With this approach the scintillator is oriented so that it is thicker in the neutron direction, thereby increasing the probability of an interaction and helping to contain the long proton recoil tracks. Also, there could be a substantial cost saving for arrays, since only one phototube is required for each meter long scintillator.

Figure 13a shows the fraction of the emitted light that has reached the phototube as a function of time after the neutron enters the scintillator.

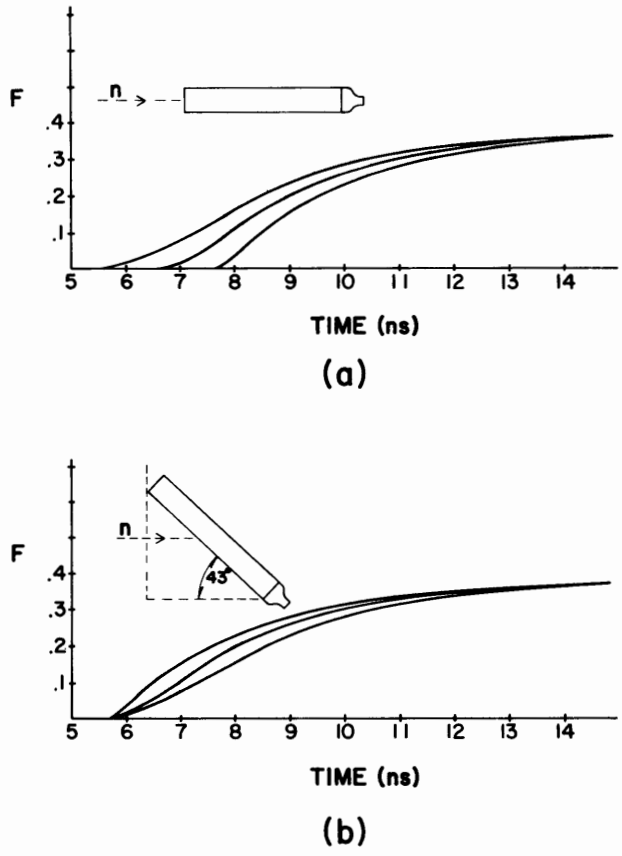

Figure 13.

(a) The curves show the fraction of forward emitted light that has reached the phototube by time t, measured from when the neutron crosses the plane through the front face of the scintillator. The parameters used are: length of scintillator = 1 m, index of refraction = 1.6, phosphor decay constant = 2.4 ns, neutron energy = 100 MeV. The three curves are for scintillations at the front, middle and back of the scintillator.

(b) This shows how time compensation is achieved by tilting the scintillator. The calculation is the same as for Fig. 13a except for the tilt.

The calculation is for 1 m length and neutron energy of 100 MeV. The three curves are for scintillations at the front, middle, and back of the scintillator. The curve for the back starts later because the difference in light paths for different emission angles is less. Figure 13b shows how the time origins of the light pulses can be made to coincide by tilting the scintillator. Compensation for the variations in rise time is then achieved with quadratic extrapolated zero timing that makes use of the approximately parabolic shape of the pulses near their origins.

The best time resolution that has been achieved in real neutron spectra at IUCF is about 0.8 ns FWHM and this has been achieved with tilted detectors, mean timing, and small detectors alike.

Two techniques were used to measure the detector efficiency at energies near 100 MeV. In one measurement neutrons from $^{7}Li(p,n)^{7}Be$ were counted during proton bombardment of a fresh target with E_p = 120 MeV. Afterwards, the number of ^{7}Be nuclei created was inferred from an absolute gamma count of the ^{7}Be in the target. The angular distribution was measured separately. In another measurement neutrons from $^{12}C(p,n)^{12}N(g.s.)$ were counted. The cross section was calculated from a measurement of $^{12}C(p,p')^{12}C(15.1\ MeV)$ and the assumption of isospin conservation. Both methods yielded the result that the effective solid angle of the tilted detector is equivalent to that subtended by an area of 32% of cross sectional face (15 cm x 15 cm).

*Collaborative effort by outside user groups: C. Goodman (ORNL); B. Anderson, A. Baldwin, J. Knudson, R. Madey and T. Witten (Kent State Univ.); D. Bainum and J. Rapaport (Ohio Univ.); C. Goulding and M. Greenfield (Florida A&M Univ.); D. Lind and C. Zafiratos (Univ. of Colo.); S. Schery (Texas A&M Univ.); C. Foster (IUCF).

1) C.D. Goodman, J. Rapaport, D.E. Bainum, and C.E. Brient, accepted for publication in Nucl. Inst. and Meth.

2) C.D. Goodman, J. Rapaport, D.E. Bainum, M.B. Greenfield, and C.A. Goulding, IEEE Trans. on Nucl. Sci. NSS-25, NO. 1, Feb. 1978.

Development of Future Facilities

QQSP Pion Spectrograph

In order to increase the efficiency of data collection in reactions which produce charged pions, H. Enge of Deuteron Inc. was commissioned to design a spectrograph of modest energy resolutions with large solid angle, large momentum bite, and short flight path. The spectrograph system (QQSP) consisting of two quadrupole magnets and a split dipole magnet is shown schematically in Figure 14. The basic properties of the system are summarized in Table 8.

A contract has been awarded to Alpha Scientific, Inc. of Hayward, Ca. to carry out the engineering design and fabrication of the magnets. Delivery of the system is anticipated for the end of summer, 1978. Installation of the system in the target room shared with the 64" scattering chamber (see Figure 3) will then take place in the last quarter of 1978.